LIGHT DIFFRACTION BASED OVERLAY MEASUREMENT

J. Bischoff * , R. Brunner, J. Bauer and U. Haak
(JB, RB Carl Zeiss Jena GmbH, JB, UH IHP Frankfurt/O.)
Carl-Zeiss-Promenade 10, 07745 Jena / Germany

ABSTRACT

Optical overlay measurement methods are very effective since they are rapid and non-destructive. Imaging techniques need sophisticated image processing and suffer from the wave-optical resolution drawback. Presently, leading edge devices are offered with 5 through 10 nm measuring accuracy. In this paper a method is proposed that relies on the diffraction of a probing laser beam at a periodic reference pattern. This special pattern is implemented in the circuit layout. After the resist patterning of the second of two consecutive layers, the diffraction at the resulting net grating is measured. If an appropriate grating design is chosen, the misalignment error can be directly extracted from the diffraction efficiency. In order to obtain a strong diffraction signal and thus a sufficient signal-to-noise ratio optimum grating designs have been computed by means of rigorous diffraction modeling. Experimental results supported by rigorous modeling suggest that this technique could have the potential to meet next generation overlay accuracy requirements.

Keywords: Overlay measurement, stepper qualification, diffraction, diffraction grating

1. INTRODUCTION

Box-in-box or frame-in-frame techniques [1,2] are the state of the art in present overlay measurement. These methods are based on the evaluation of images recorded with a CCD-camera by means of sophisticated image processing algorithms. Essentially, the decentering of a frame or box patterned in one layer has to be determined in relation to a frame or box generated during a foregoing patterning cycle. Under optimum conditions accuracies of 5 through 10 nm can be achieved. Thus the approach fully meets the requirements of today's lithography.

However, there are also some drawbacks. First, due to the small depth of focus associated with high-resolution imaging optics the focus must be put on one layer. Hence, the image of the second layer overlay mark may be appear blurred. To overcome this issue at least to images with different focus settings have to be taken. Second, the image contrast depends on the material properties of the particular layer as well as on the probing wavelength [3]. In the worst case this can lead to complete failures of the overlay metrology tool. And third, non-symmetric edge deposition may occur caused by the self shadowing of mark depth. This effect is called wafer-induced-shift. Special overlay measurement mark designs are recommended to avoid this error source [4].

Another concern is the further development of measurement accuracy requirements. The Sematech roadmap predicts the 70 nm critical dimension (CD) node for the year 2004. It will be associated with an overlay budget of about 10 to 20 nm resulting in a required overlay tool precision of 1.3 nm. Probably, these requirements are beyond the limits of optical imaging based tools. Recent publications show that the box in box techniques may become insufficient with shrinking device geometry [2].

2. BASIC PRINCIPLE

In spite of the high lateral and vertical resolution of non-optical techniques such as scanning electron microscopy and atomic force microscopy applied to overlay metrology, optical methods have the crucial advantage of being rapid and non-destructive. Light based metrology principles can be maintained if the diffraction is purposely applied to get more information about the causing scatterer. This has been shown successfully in the field of CD-metrology where the so-called optical scatterometry [5-7] and related spectral methods [8] have been evolved to serious competitors.

Diffractive zone plate alignment marks have been proposed by Feldman and White[9]. We propose an overlay measurement technique that makes use of the defined diffraction of light. This technique can be applied both for the stepper evaluation and for the overlay measurement of consecutive patterning layers.

As for the stepper qualification, the following scenario is proposed. After being coated with photoresist the wafer is exposed with the mask containing a special diffractive overlay mark. This overlay mark comprises a simple transmission grating with a line-to-space-ratio greater than 1:1 for a positive resist and less than 1:1 for negative one. (On a first glance, a factor 3, that is to say either 3:1 (positive) or 1:3 (negative) seems to be a reasonable choice which results as can be seen later to a duty cycle of 1:1 in the overlay pattern to be measured.)

After printing the mask, the latent overlay grating has a period p on the wafer. We call this first grating primary grating. The inverse of the grating period can be considered as a spatial frequency 1/p. In a second step, a stepper repositioning is done including an additional offset of exactly half a period of the overlay grating. Then, the wafer is exposed again with the same dose as before and thereafter, the resist is developed. The further procedure shall be exemplified with the positive resist process. In case of accurate alignment, the spaces (or lines, respectively in case of applying a negative resist) of the second exposed grating or secondary grating fit exactly in the larger lines of the first one. The result is a grating with the doubled spatial frequency 2/p. If the second exposure is misaligned caused by the stepper tool error the spaces of the second grating are shifted either to the right or to the left in relation to those of the primary grating. In other words the resulting grating keeps the period p. Figure 1 shows a schematic example of a negative resist and figure 8 contains cross sectioning micrographs of a overlay pattern printed in positive resist.

Now the overlay measurement can be performed by illuminating the overlay mark with a laser beam at normal incidence. Choosing an appropriate wavelength, the first order diffraction disappears if the misalignment approaches zero due to the doubling of the grating frequency. The right wavelength-to-period ratio can be found by means of the well known grating equation:

$$\sin\theta_m = m \cdot \frac{\lambda}{p}$$

with m being the diffraction order, θ_m the angle of this order and λ the wavelength of the probing beam. In order to allow the first diffraction order to propagate for a period p and suppress it for half the period p/2, the wavelength-to-period ratio has to be chosen between:

$$0.5 < \frac{\lambda}{p} < 1$$

For instance, a He-Ne laser with 633 nm is suited for a basic grating period of 1 micron. In this case, the first order reflection is deflected at about 39.3 degrees from the normal direction.

Our next consideration shall be devoted to the question whether this principle can be transferred to the overlay measurement between consecutive patterning cycles. To this end, let's have a closer look at the underlying procedure of overlay measurement. Shortly, the procedure runs as follows. First, a primary grating is generated in the first patterning cycle. Depending on the particular technology step this primary grating can be etched for example in poly-silicon or oxide. After completing this technology step, the next patterning cycle is launched with the resist coating step. The reticle for the photolithographic exposure contains the same overlay grating like

the reticle used in the foregoing patterning step, but it is displaced by half a grating period on the mask layout. Then, the wafer is developed and the secondary grating is printed in photoresist.
Evidently, the straightforward principle explained above cannot be directly applied to overlay measurement since the two patterns are usually made of different materials, e.g., resist and silicon or oxide. Thus the resulting grating originating from the superposition of the primary and secondary grating will not double its frequency even in the case of perfect overlay. However, it may become symmetric. This means that the plus and the minus first order will provide the same efficiency for ideal alignment. Hence, the basic principle can be maintained by measuring the difference between the plus and minus first diffraction order.

3. MODELING

3.1 Theory

Generally, the relation between overlay error and diffraction signal will be non-linear. Therefore the diffraction response versus overlay error must be calculated as accurate as possible. Moreover, due to the very fine geometry, the light polarisation has to be taken into consideration. This can only be done by full electromagnetic approaches. An overview over the most widely accepted methods is given for instance in [10]. The Rigorous Coupled Wave Approach (RCWA)[11,12] which adheres to the modal methods with Fourier expansion has been evolved to one of the most versatile and robust algorithms for the diffraction computation of multilayer gratings. A characteristic feature of the RCWA is the so-called slicing where the grating profile is decomposed in a number of thin slices in which the refraction index is independent on the normal direction. Basically, this method relies on the transformation of Maxwell's equations within a slice into a system of differential equations for the transversal field components. Then, these equations are Fourier factorised and solved by means of an Eigenvector/Eigenvalue decomposition. And eventually, the elementary solution matrices in every slice are coupled recursively to connect cause and response fields on the front side and back side of the multilayer system. This procedure was implemented numerically in the UNIGIT®-code.

3.2 Modeling Results

Now we are going to verify the qualitative arguments made in section 2 by means of numerical simulations. First, the stepper qualification, i.e., the resist in resist grating shall be considered. Here, two cases shall be investigated – a resist (Shipley positive resist DUV 210) grating with a period of 1 micron that is illuminated with a 633 nm beam and a resist grating with 600 nm period probed with 442 nm wavelength (He-Cd laser). The mean duty cycle (line-to-space ratio) was set to 3:1. To investigate the impact of the duty cycle, additional computations were performed with increased and decreased ratios. In all cases a resist thickness of 420 nm was assumed corresponding to the IHP resist process. Then the misalignment was changed gradually from –100 nm through +100 nm and the diffraction efficiency of the first order in reflection was calculated for both polarisation cases namely TE and TM. The results are depicted in figures 3a through 3c. Figure 3a shows the TE-polarisation case and figure 3b shows the TM-case for the 1 micron grating illuminated with 633 nm. Here, the spacewidth s of the basic grating served as a parameter. It was varied from 0.2 through 0.3 microns (which corresponds to duty ratios of 4:1 and 2.3:1). For the definition of the spacewidth see figure 8.

From these simulations the following conclusions can be drawn:

- First, the feasibility of the basic principle explained in section 2 is confirmed. That is to say, the first order diffraction drops to zero in the state of best alignment.
- Second, a non-linear parabolic dependence is observed between first order diffraction efficiency and alignment error. The slope of the curve is zero at zero error. This means low sensitivity of the method at small tool errors. Having an efficiency value of 0.002% at 1 nm and of about 10 at 100 nm misalignment, the required dynamic range is about $5 \cdot 10^3$.
- Third, working with TM-polarised light gives a stronger signal compared to illumination with TE-polarisation, although in the best case (s = 0.3 µm) the modulation is nearly equal. However, in general the polarisation impact is also dependent on other factors such as the resist thickness.

- Fourth, the best sensitivity is expected for an increased width of the spaces s (low duty ratio).

Next, the overlay measurement technique shall be investigated numerically. Since the Poly-silicon layer is particular critically we focused our efforts on this technology step. In contrast to the stepper qualification we considered the alignment of a resist line grating relative to a previously patterned Poly-Si Grating. The cross section of the complete multilayer stack is depicted in figure 4. The ARC layer is necessary for the second resist patterning thus covering the Poly-Si lines. It has a thickness of 20 nm at the bottom and of 40 nm at the top of the Poly-Si lines. Below the ARC a 5 nm thick gate oxide layer was deposited. The Poly-Si lines are 200 nm in height whereas the resist lines are 420 in height. Figure 5 shows the computed diffraction efficiencies for the +1. diffraction order in reflection for normal incidence of a 633 nm laser beam. The -1. order curves are not depicted since they are mirrored on the y-axis due to the inherent symmetry of the arrangement. Obviously, the curves do not drop to zero for diminishing overlay error. However, if we consider the difference between the +1. and the -1. order the optimum constellation observed from the resist in resist case can be retained, i.e., the signal can be forced to zero at zero alignment error. Moreover, the difference signals (bold curves) show two benefits:

- First, the curves are pretty linear. This facilitates the calibration of the overlay sensor. Furthermore, the measurement accuracy is expected to better than in the resist in resist case. The required dynamic range is reduced to 10^2 (related to an alignment error range from 1 nm through 100 nm).
- Second, the signal changes its sign with a zero crossing. In this way, the direction of the misalignment can be derived, i.e., a negative signal corresponds to a negative shift and a positive one to a positive shift.
- Third, a stronger signal sensitivity is observed for TE polarised light.

4. EXPERIMENTAL

So far, we proved the feasibility of the proposed diffractive overlay measurement by means of rigorous modeling. In this section, some of the results shall be verified by experiment. Again the two cases, stepper qualification and Poly-Si overlay shall be investigated. Two 8 inch silicon wafers were prepared - one with a resist pattern and one with a developed resist pattern above an underlying Poly-Si layer. The photolithographic exposure was performed with a Nikon DUV stepper. Here, we used a special mask design that was developed for the particular application of generating test patterns for the optical CD metrology. Among other patterns the mask contains line/space patterns with line/space ratios ranging from 1:4, 1:3, 1:1, 3:1 to 4:1 and with 1 µm pitch after printing onto the wafer. In the second exposure, the reticle was offset perpendicular to the grating lines. In addition to the basic offset of a half grating period (500 nm), an overlay error simulating offset was chosen ranging from -100 nm in steps of 25 nm through +100 nm. This overlay error was assigned to the rows on the wafer, i.e., the first row corresponds to +100 nm misalignment and so on. Eventually, according to the local secant across the wafer three (top and bottom) to nine (center) exposure fields with identical nominal displacement were printed onto the wafer.

Following, the actual alignment error was measured by means of CD scanning electron microscopy (SEM). Figure 6 presents some representative examples of SEM-micrographs. It contains two different alignment states out of 9 possible ones for the resist in resist pattern (the dark areas are the spaces). In the frame of this paper, the central column of exposure fields was selected for the investigations. Further evaluations of the neighboured fields must be adjourned to a later date. From these more comprehensive measurements a statistical evaluation can be derived. While the left hand side shows the secondary grating displaced relative to the primary grating by a nominal value of 75 nm, the right hand side presents the best case with no alignment error. This corresponds to the anticipated doubling of the grating frequency. The displacement measurements by means of these micrographs also reveal that there are deviations from the nominal values. Essentially, these deviations shown in table 1 are caused by the tool error of the stepper.

Nominal Displacement in nm	- 100	-75	-50	-25	0	+25	+50	+75	+100
Measured Displacement in nm	-125.5	-80	-49	-23.5	+5	+25.5	+50	+73	+104.5

After examining the overlay patterns by means of the CD-SEM, the optical measurements were performed in the next step. The experimental arrangement corresponds mainly to the schema depicted in figure 2. The overlay patterns having dimensions of 1 by 3 mm were illuminated with a 633 nm laser beam focused to about 0.8 mm in diameter on the wafer surface. Then, the diffracted light was measured using a photosensitive element. Several measurements were performed per site with repositioning the sample. In addition, the incident intensity was measured each time before moving to the next measuring site. The diffraction efficiency is then obtained from the intensity ratio (diffracted to incident energy). Last, the measured diffraction values were compared with the modeling results. Figure 7 exhibits the results for the resist in resist grating. Obviously, the agreement between SEM-measurement and optical diffraction measurement is quite good. Some slight deviations might arise from local overlay variations within the measuring field, from photometric measurement uncertainties and from profile slopes differing from the 90 degrees assumed for the modeling.

Finally, cross sectioning preparations were made from the test wafer. Generally, the analysis of these micrographs confirmed the results obtained from the top down measurements. Besides, these micrographs served as input profiles for the modeling. Figure 8 shows two alignment states (LHS misaligned, RHS aligned) for the resist in resist case and figure 9 for the resist in Poly-Si grating.

5. CONCLUSION

An alternative method for overlay metrology in microtechnology was presented. This method is based on the light diffraction at grating patterns shifted against each other. Beside overlay metrology, stepper alignment qualification might be another important application. The basic principle of the proposed method relies on the symmetry of the resulting overlay mark in case of ideal alignment. Here it was shown that either the diffraction efficiency in the first order (resist in resist pattern) or the difference between the two first orders (resist in non-resist pattern) has to be used as signal. The physical considerations were examined by means of rigorous modeling. Besides, optimum overlay patterns were derived from the simulations. Finally, the proof of the experimental feasibility was given. The obtained results are very encouraging. Experimental results show good conformity with the mathematical modelling. Essentially, the method seems to have the potential for overlay measurement accuracy down to 1 nanometer. Much more work is necessary to obtain more clarity about the practicability and attainable accuracy of the proposed technique.

ACKNOWLEDGEMENT

This work was financially supported by the Thuringia State Ministry of Science, Research and Arts (TMWFK) under Grant No. B509-99033. Besides, we like to thank Mrs. Naumann from IHP Frankfurt/O. for the SEM-preparations.

REFERENCES

1. S. H. Fox, R. M. Silver, E. Kornegay and M. Dagenais, "Focus and edge detection algorithms and their relevance to the development of an optical overlay calibration standard," Proc. SPIE **3677**, pp. 95-106, 1999.

2. V. C. Jai Prakash and C. J. Gould," Comparison of optical, SEM, and AFM overlay measurement," Proc. SPIE **3677**, pp. 229-238, 1999.

3. J.-S. Han, K. Hak, J.-L. Nam, M.-S. Han, S.-K. Lim, S. D. Yanowitz, N. P. Smith and A. M. Smout, "Effects of illumination wavelength on the accuracy of optical overlay metrology," Proc. SPIE **3051**, pp. 417-425, 1997.

4. J. Yang, S. B. Lee, S.-C. Oh, H. Huh and S.-B. Han, "Novel design of WIS-free overlay measurement mark," Proc. SPIE **3998**, pp. 764-772, 2000.

5. J. R. McNeil, S. S. H. Naqvi, S. M. Gaspar et. al., “Scatterometry applied to microelectronic processing,” Microlithography World, pp. 16-22, Nov./Dec. 1992.

6. J. Bischoff, J. Bauer, U. Haak, L. Hutschenreuther and H. Truckenbrodt, “Optical scatterometry of quarter micron patterns using neural regression,” Proc. SPIE **3332**, pp. 764-772, 1998.

7. S. A. Coulombe, B. K. Minhas, C. J. Raymond, S. S. H. Naqvi and J. R. McNeil, “Scatterometry measurement of sub-0.1 µm linewidth gratings,” J. Vac. Sci. Technol. B **16**, pp. 80-87, 1998.

8. X. Niu, N. Jakatdar, J. Bao, C. Spanos and S. Yedur, "Specular Spectroscopic Scatterometry in DUV Lithography," Proc. SPIE **3677**, pp. 159-168, 1999.

9. M. Feldman, A. D. White and D. L. White, "Method and apparatus for aligning mask and wafer members," U.S. Patent 4326805, 1982.

10. J. Bischoff, ”Beiträge zur theoretischen und experimentellen Untersuchung der Lichtbeugung an mikro-strukturierten Mehrschichtsystemen,” Habilitationsschrift (Thesis habil.), TU Ilmenau/ Germany 2000.

11. M. G. Moharam, D. A. Pommet, E. B. Grann, and T. K. Gaylord, “Stable implementation of the rigorous coupled-wave analysis for surface-relief gratings: enhanced transmittance matrix approach,” J. Opt. Soc. Am. **A 12**, pp. 1077-1086, 1995.

12. Lifeng Li, “Multilayer modal method for diffraction gratings of arbitrary profile, depth, and permittivity,” J. Opt. Soc. Am. **A 10**, pp. 2581-2591, 1995.

- Correspondence: email: j.bischoff@zeiss.de; phone: +493641 64 2850

FIGURES

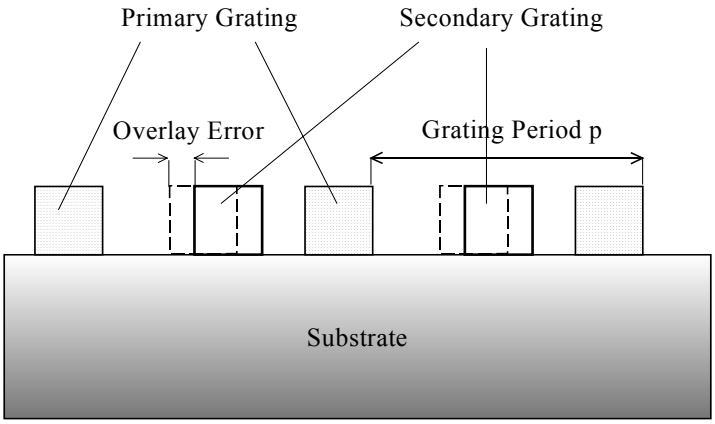

Figure 1: Schematic layout of the diffractive overlay mark

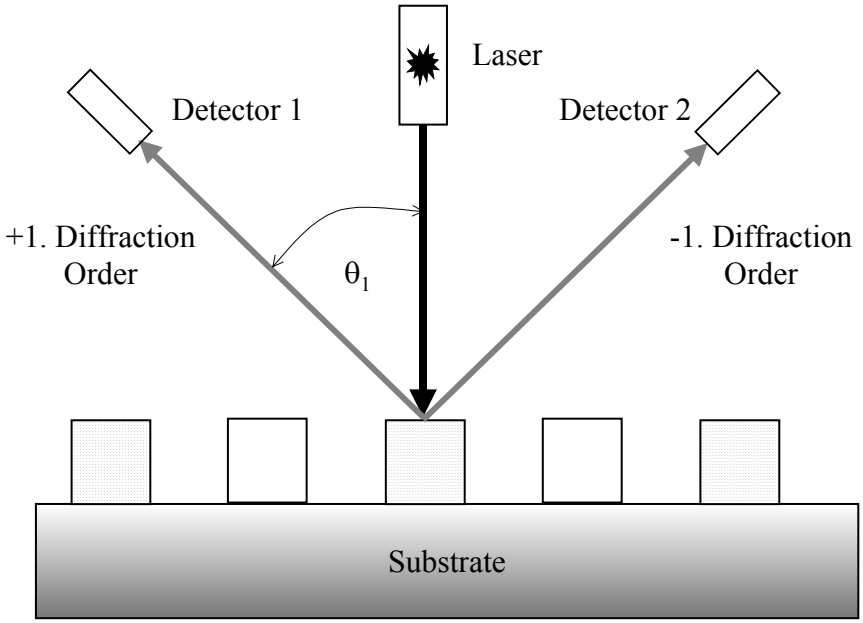

Figure 2: Experimental arrangement for the overlay measurement using diffractive marks

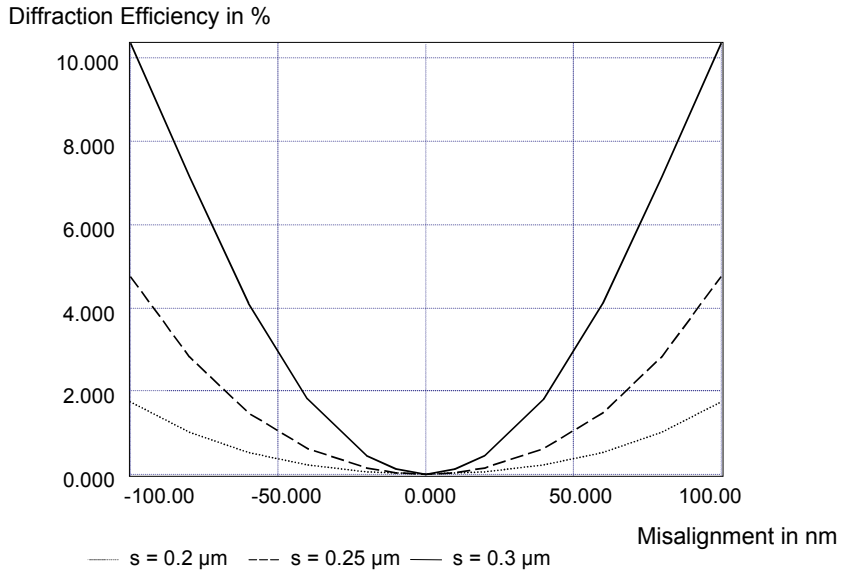

Figure 3a: Simulation of the +1. diffraction order efficiency vs. lateral misalignment for the 1 µm grating probed with 633 nm in TE-polarized light with the spacewidth s of the basic grating as parameter

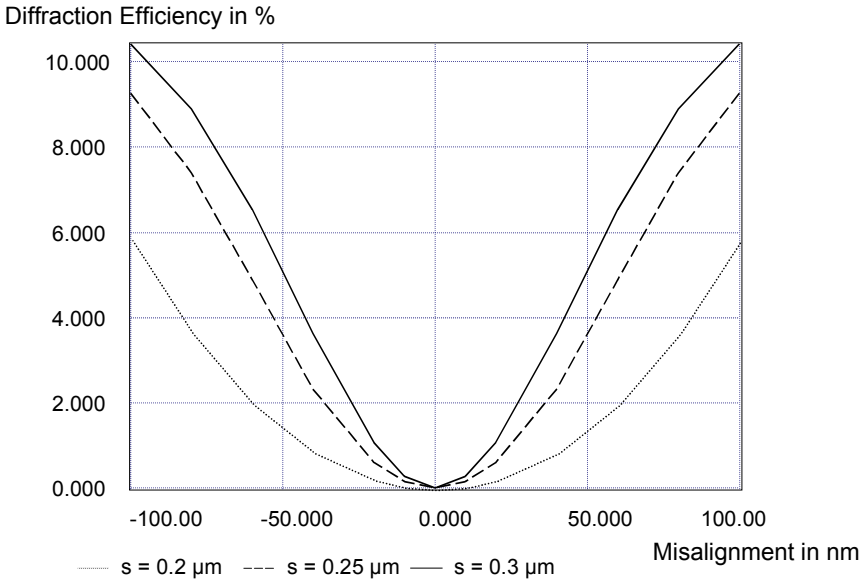

Figure 3b: Same as Fig. 3a, but TM-polarization

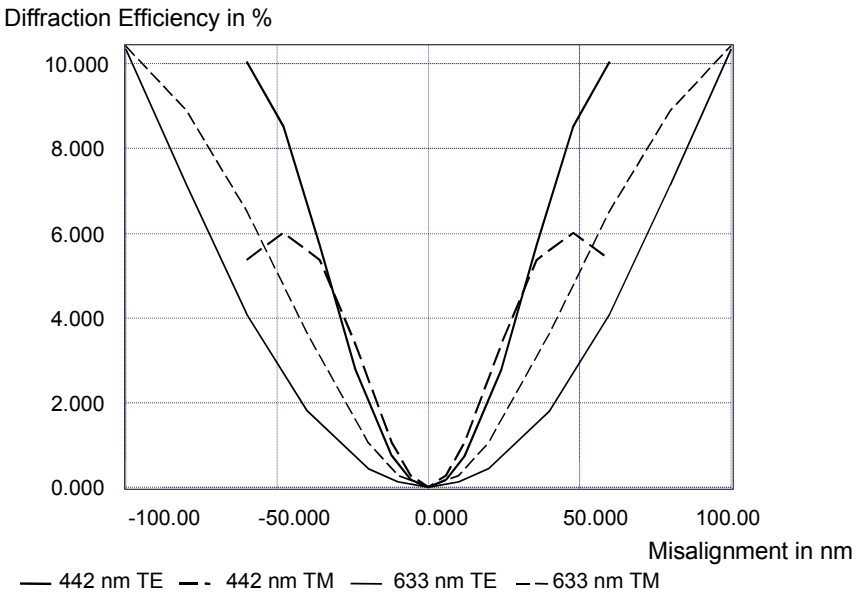

Figure 3c: Comparison of the response (1. order efficiency) for a 1 µm pitch grating probed with λ = 633 nm (TE - slim solid line, TM - slim dashed line) with a 600 nm grating pitch probed with 442 nm (TE - bold solid line, TM - bold dashed line)

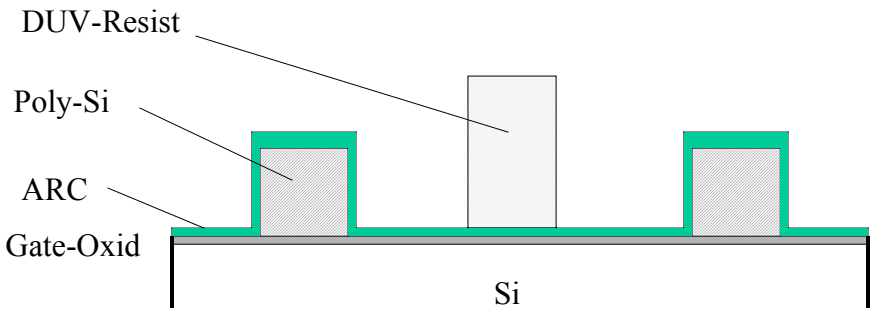

Figure 4: Schematic illustration of the Poly-Si layer overlay pattern after resist development of the following patterning cycle

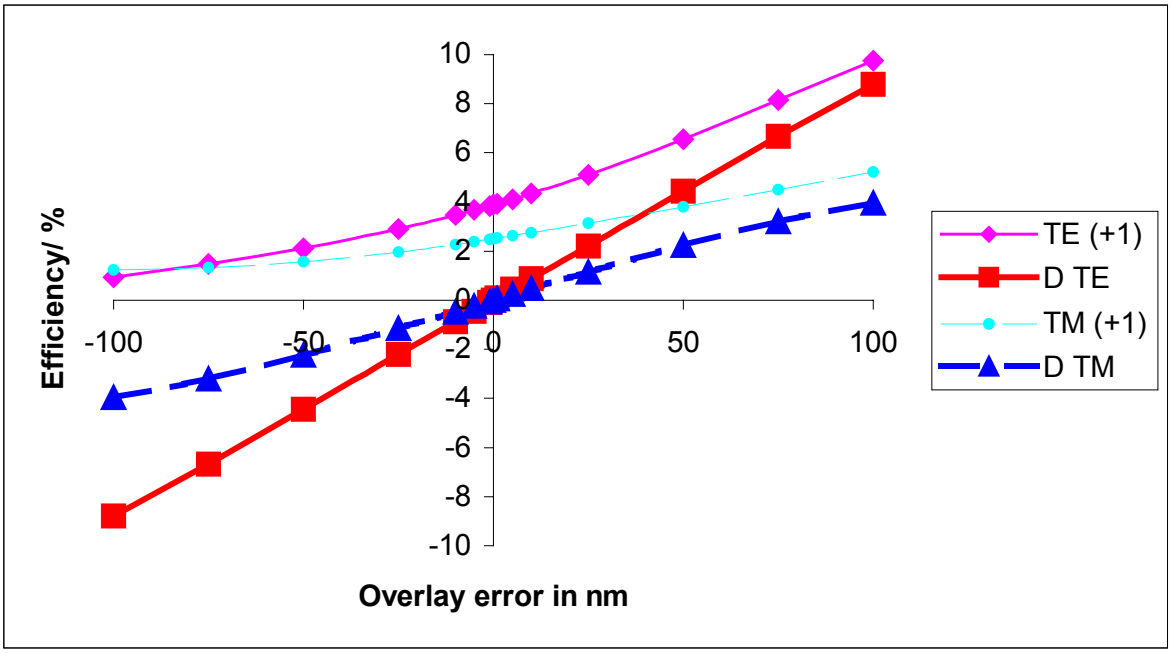

Figure 5: Simulation of the detector response for the Poly-Si overlay pattern presented in figure 4. The slim lines show the +1. order diffraction efficiencies (the -1. order are mirrored on the y-axis thus having a negative slope) and the bold lines present the difference D between the +1. and the -1. order (solid lines -TE, dashed lines - TM).

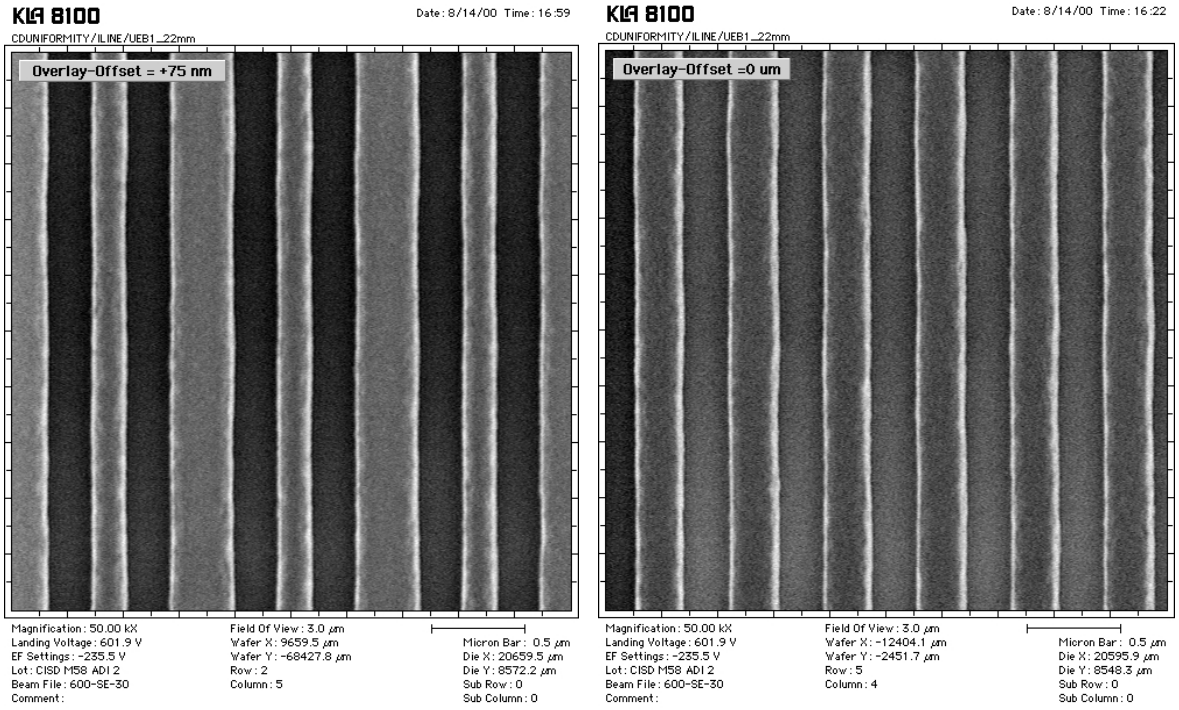

Figure 6: Top down view of the resist in resist overlay pattern (LHS: with nominal displacement of 75 nm, RHS: without overlay error, i.e., with no nominal displacement)

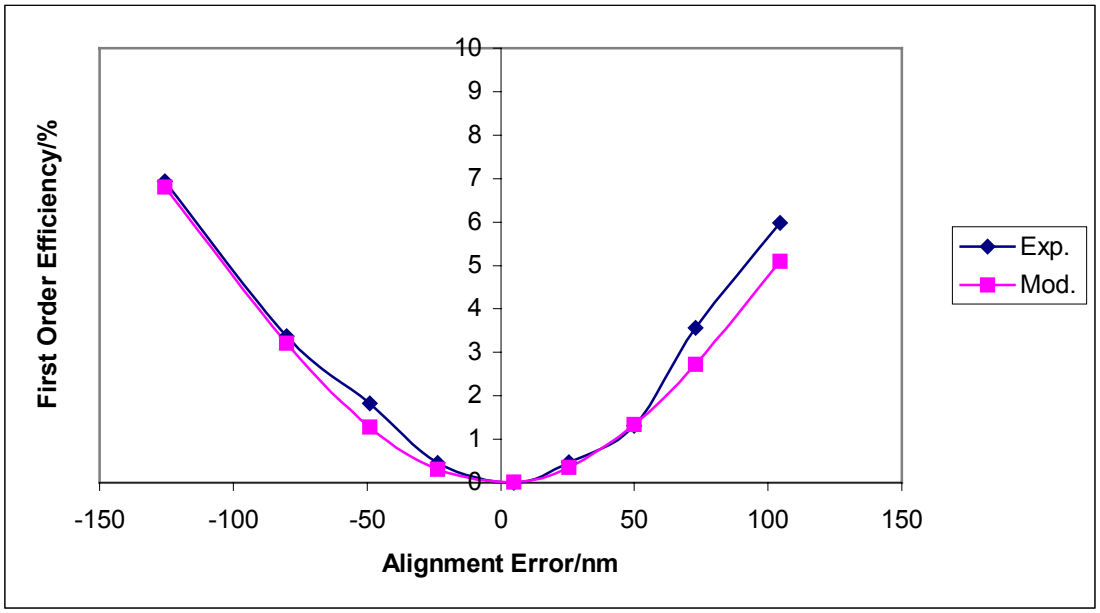

Figure 7: First order diffraction efficiency (TE polarisation) for the 1 μm resist in resist grating - measured (diamonds) versus modeled (squares).

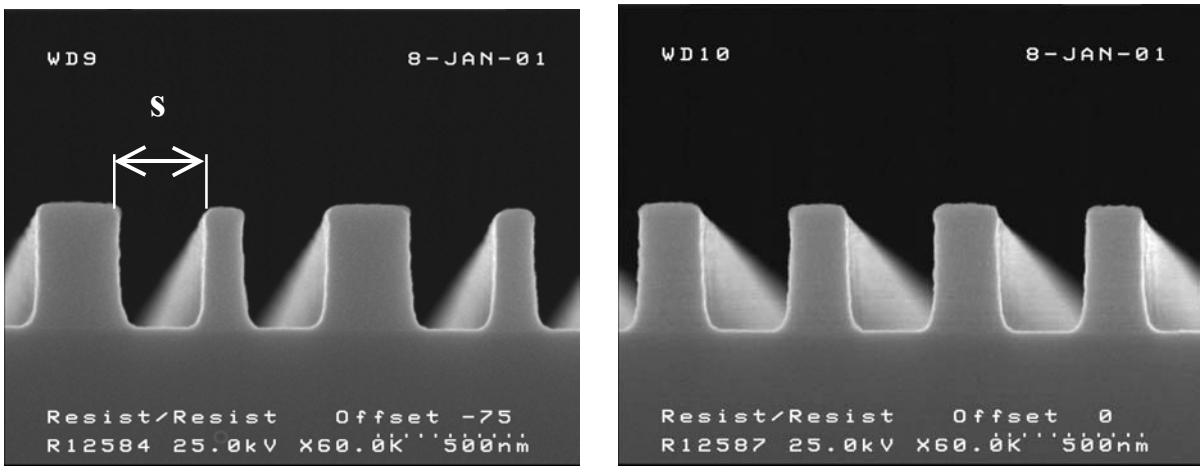

Figure 8: Cross section of the resist in resist overlay pattern (LHS: with nominal displacement of 75 nm, RHS: without overlay error, i.e., with no nominal displacement)

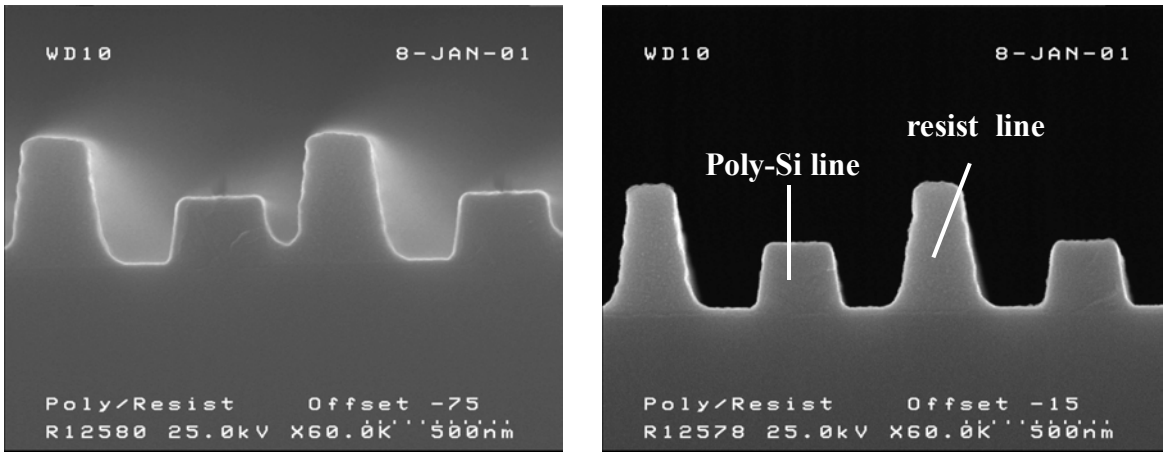

Figure 9: Cross section of the resist in Poly-Si overlay pattern (LHS: with nominal displacement of 75 nm, i.e., the resist lines are shifted to the left in relation to the Poly lines by about 75 nm, RHS: nearly perfect alignment).